Chaos Induced by Quantization

Takaomi Shigehara, Hiroshi Mizoguchi, Taketoshi Mishima
Department of Information and Computer Sciences, Saitama University, Shimo-Okubo, Urawa, Saitama 338-0825, Japan

Taksu Cheon
Laboratory of Physics, Kochi University of Technology, Tosa Yamada, Kochi 782-8502, Japan

(January 28, 1998)

In this paper, we show that two-dimensional billiards with point interactions inside exhibit a chaotic nature in the microscopic world, although their classical counterpart is non-chaotic. After deriving the transition matrix of the system by using the self-adjoint extension theory of functional analysis, we deduce the general condition for the appearance of chaos. The prediction is confirmed by numerically examining the statistical properties of energy spectrum of rectangular billiards with multiple point interactions inside. The dependence of the level statistics on the strength as well as the number of the scatterers is displayed.

KEYWORDS: wave chaos, quantum mechanics, pseudointegrable billiard, point interaction, functional analysis

I. INTRODUCTION

The billiard is a suitable tool for examining generic features of dynamical systems. This is because, in spite of its simplicity, it covers the wide range of dynamical behaviors, going from the most regular (integrable) to the most irregular (chaotic) depending on its shape. Pseudointegrable [1] billiards discussed in this paper is obtained by putting point scatterers into an integrable billiard. Their dynamical behavior is somewhat trivial in classical mechanics. A classical point particle never hits a point scatterer. More precisely, the set of trajectories of a point particle which hit point scatterers is of measure zero in the classical phase space. Thus we may neglect point obstacles in classical mechanics. However, the situation is drastically changed in quantum mechanics. Owing to the uncertain principle, the point particle gains a "size" and as a result, there might be a possibility of its hitting point scatterers. Our purpose is to show this is in fact the case and to clarify the condition for its occurrence. In order to emphasize that such phenomena originate from quantum effects, they might be called *wave chaos* [2].

A particular case of a single scatterer located at the center of a rectangular billiard has been discussed in details elsewhere [3]– [5]. We generalize the formulation and derive the transition matrix in case of multiple scatterers. Based on this, a new numerical evidence for the existence of wave chaos is exhibited. We observe that the "degree" of chaos strongly depends on the number of the scatterers.

The paper is organized as follows. In Sect.2, we briefly mention the measure of chaos in quantum mechanics, which is described by statistics of energy levels. The quantum-mechanical treatment of point scatterers is discussed in Sect.3. In spite of seeming simplicity of the problem, a somewhat complicated argument based on self-adjoint extension is needed. In Sect.4, we clarify the condition for the appearance of wave chaos and its validity is confirmed by numerical experiments with a rectangular billiard in Sect.5. The paper is summarized in Sect.6.

II. QUANTUM-MECHANICAL MEASURE OF CHAOS

Although no mathematical proof exists, it is widely conjectured [6] that the statistical properties of quantum energy spectrum directly reflect the dynamical nature of the corresponding classical system. Generic integrable systems obey Poisson statistics, while generic chaotic systems are described by the predictions of the Gaussian orthogonal ensembles (GOE) [7]. One of such statistical measures is the nearest-neighbor level spacing distribution $P(S)$, which is defined such that $P(S)dS$ gives the probability to find the spacing between any two neighboring energy eigenvalues in the interval $(S, S+dS)$. Depending on the dynamical property of classical system, $P(S)$ takes a form

$$P(S) = \begin{cases} \exp(-S), & \text{(integrable)}, \\ \dfrac{\pi S}{2}\exp(-\dfrac{\pi S^2}{4}), & \text{(chaotic)}. \end{cases} \tag{1}$$

The degeneracy of eigenvalues frequently happens in integrable systems, while it hardly occurs in chaotic systems. Another convenient statistics is the spectral rigidity

$$\Delta_3(L) = \left\langle \min_{A,B} \frac{1}{L} \int_{E-L/2}^{E+L/2} \left(N(E') - AE' - B\right)^2 dE' \right\rangle_E , \tag{2}$$

where $N(E)$ is the staircase function which counts the number of eigenstates below energy E. The brackets $\langle\cdot\rangle_E$

signify the average with respect to the energy in the energy region under consideration. The $\Delta_3(L)$ statistics represents the average of the least square deviation of the staircase function $N(E)$ from the best straight line fitting it in some intervals of length L. It takes a form

$$\Delta_3(L) = \begin{cases} \dfrac{L}{15}, & \text{(integrable)}, \\ \dfrac{1}{\pi^2}(\ln L - 0.0687), & \text{(chaotic)}, \end{cases} \tag{3}$$

depending on the dynamical property.

III. FORMULATION

We first consider a quantum point particle of mass M moving freely in a two-dimensional bounded region (billiard) S. Let us denote the area of S by the same symbol. We impose the Dirichlet boundary condition so that wave functions vanish on the boundary of S. The eigenvalues and the corresponding normalized eigenfunctions are denoted by E_n and $\varphi_n(\vec{x})$ respectively;

$$H_0\varphi_n(\vec{x}) \equiv -\frac{\nabla^2}{2M}\varphi_n(\vec{x}) = E_n\varphi_n(\vec{x}). \tag{4}$$

The Hamiltonian H_0 is the kinetic operator in $L^2(S)$ with domain $D(H_0) = H^2(S) \cap H_0^1(S)$ in terms of the Sobolev spaces. The Green's function of H_0 is written as

$$G^{(0)}(\vec{x},\vec{y};\omega) = \sum_{n=1}^{\infty} \frac{\varphi_n(\vec{x})\varphi_n(\vec{y})}{\omega - E_n}, \tag{5}$$

where ω is the energy variable. The average level density of the system is given by

$$\rho_{av} = \frac{MS}{2\pi}, \tag{6}$$

which is energy-independent.

We now place a single point scatterer at $\vec{x}_1$ inside the billiard. The most naive manner for this purpose is to define the scatterer in terms of the Dirac's delta function;

$$H = H_0 + v\delta^{(2)}(\vec{x} - \vec{x}_1). \tag{7}$$

However, the Hamiltonian H is not mathematically sound. This can be seen from the eigenvalue equation of H, which is reduced to

$$\sum_{n=1}^{\infty} \frac{\varphi_n(\vec{x}_1)^2}{\omega - E_n} = v^{-1}. \tag{8}$$

Since the level density is proportional to $E^{(d-2)/2}$ in spatial dimension d, the infinite series in Eq.(8) does not converge for $d \geq 2$.

To handle the divergence, a scheme for renormalization is called for. The most general scheme is given by the self-adjoint extension theory of functional analysis [8]. We first consider in $L^2(S)$ the nonnegative operator

$$H_{\vec{x}_1} = -\left.\frac{\nabla^2}{2M}\right|_{C_0^\infty(S-\vec{x}_1)} \tag{9}$$

with its closure $\bar{H}_{\vec{x}_1}$ in $L^2(S)$. Namely, we restrict $D(H_0)$ to the functions which vanish at the location of the point scatterer;

$$D(\bar{H}_{\vec{x}_1}) = \{\psi(\vec{x}) \in D(H_0) | \psi(\vec{x}_1) = 0\}. \tag{10}$$

By using integration by parts, it is easy to prove that the operator $\bar{H}_{\vec{x}_1}$ is symmetric (Hermitian). But it is not self-adjoint. Indeed, the equation for the adjoint of $\bar{H}_{\vec{x}_1}$

$$\bar{H}^*_{\vec{x}_1}\psi_\omega(\vec{x}) = \omega\psi_\omega(\vec{x}), \quad \psi_\omega \in D(\bar{H}^*_{\vec{x}_1}), \tag{11}$$

has a solution for $Im\ \omega \neq 0$ [9];

$$\psi_\omega(\vec{x}) = G^{(0)}(\vec{x},\vec{x}_1;\omega), \quad \vec{x} \in S - \vec{x}_1, \tag{12}$$

indicating

$$\begin{aligned} D(\bar{H}^*_{\vec{x}_1}) &= D(\bar{H}_{\vec{x}_1}) \oplus N(\bar{H}^*_{\vec{x}_1} - \omega) \oplus N(\bar{H}^*_{\vec{x}_1} - \bar{\omega}) \\ &\neq D(\bar{H}_{\vec{x}_1}), \end{aligned} \tag{13}$$

where $N(A)$ is the kernel of an operator A. Equation (13) means that $\bar{H}_{\vec{x}_1}$ has the deficiency indices $(1,1)$ and as a result, $\bar{H}_{\vec{x}_1}$ has one-parameter family of self-adjoint extensions H_{θ_1};

$$\begin{aligned} D(H_{\theta_1}) &= \{f | f = \varphi + c(\psi_{i\Lambda} - e^{i\theta_1}\psi_{-i\Lambda}); \\ &\qquad \varphi \in D(\bar{H}_{\vec{x}_1}), c \in \mathbf{C}, 0 \leq \theta_1 < 2\pi\}, \\ H_{\theta_1} f &= \bar{H}_{\vec{x}_1}\varphi + i\Lambda c(\psi_{i\Lambda} + e^{i\theta_1}\psi_{-i\Lambda}), \end{aligned} \tag{14}$$

where $\Lambda > 0$ is a scale mass. With the aid of Krein's formula [8], we can write down the Green's function for the Hamiltonian H_{θ_1} as

$$\begin{aligned} &G_{\theta_1}(\vec{x},\vec{y};\omega) = G^{(0)}(\vec{x},\vec{y};\omega) \\ &+G^{(0)}(\vec{x},\vec{x}_1;\omega)T_{\theta_1}(\omega)G^{(0)}(\vec{x}_1,\vec{y};\omega). \end{aligned} \tag{15}$$

In Eq.(15), the transition matrix T_{θ_1} is calculated by

$$T_{\theta_1}(\omega) = \frac{1 - e^{i\theta_1}}{(\omega - i\Lambda)c_{i\Lambda}(\omega) - e^{i\theta_1}(\omega + i\Lambda)c_{-i\Lambda}(\omega)}, \tag{16}$$

where

$$c_{\pm i\Lambda}(\omega) = \int_S G^{(0)}(\vec{x},\vec{x}_1;\omega)G^{(0)}(\vec{x},\vec{x}_1;\pm i\Lambda)d\vec{x}. \tag{17}$$

Using the resolvent equation, we have

$$T_{\theta_1}(\omega) = (v_1^{-1} - G(\omega))^{-1}, \tag{18}$$

where

$$v_1^{-1} = \Lambda \cot \frac{\theta_1}{2} \sum_{n=1}^{\infty} \frac{\varphi_n(\vec{x}_1)^2}{E_n^2 + \Lambda^2}, \tag{19}$$

$$G(\omega) = \sum_{n=1}^{\infty} \varphi_n(\vec{x}_1)^2 (\frac{1}{\omega - E_n} + \frac{E_n}{E_n^2 + \Lambda^2}). \tag{20}$$

The constant v_1 is a coupling strength of the point scatterer, the value of which ranges over the whole real number as one varies $0 \leq \theta_1 < 2\pi$. It follows from Eq.(18) that the eigenvalues of H_{θ_1} are determined by

$$G(\omega) = v_1^{-1}. \tag{21}$$

On any interval (E_m, E_{m+1}), the function G is monotonically decreasing, ranging over the whole real number. This means that the eigenvalue equation (21) has a single solution ω_m on each interval for any v_1. The eigenfunction of H_{θ_1} corresponding to an eigenvalue ω_m is given by

$$\psi_m(\vec{x}) \propto G^{(0)}(\vec{x}, \vec{x}_1; \omega_m) = \sum_{n=1}^{\infty} \frac{\varphi_n(\vec{x}_1)}{\omega_m - E_n} \varphi_n(\vec{x}). \tag{22}$$

We proceed to the case of multiple ($N \geq 1$) point scatterers. Let us denote the position of the k-th scatterer by $\vec{x}_k$. In this case, we should start with the operator

$$H_X = -\frac{\nabla^2}{2M}\Big|_{C_0^{\infty}(S-X)} \tag{23}$$

and its closure $\bar{H}_X$ in $L^2(S)$. Here we set $X = \{\vec{x}_1, \cdots, \vec{x}_N\}$. The operator $\bar{H}_X$ is symmetric (but not self-adjoint) and the equation

$$\bar{H}_X^* \psi_\omega(\vec{x}) = \omega \psi_\omega(\vec{x}), \quad \psi_\omega \in D(\bar{H}_X^*), \tag{24}$$

has the N independent solutions for $Im\ \omega \neq 0$;

$$\psi_\omega^{(k)}(\vec{x}) = G^{(0)}(\vec{x}, \vec{x}_k; \omega), \quad \vec{x} \in S - X, \tag{25}$$

$k = 1, \cdots, N$. This indicates that $\bar{H}_X$ has the deficiency indices (N, N) and as a result, it has N^2-parameter family of self-adjoint extensions in general;

$$\begin{aligned} D(H_{U,X}) = \{f | f = \varphi + \sum_{k=1}^{N} c_k(\psi_{i\Lambda}^{(k)} + \sum_{l=1}^{N} U_{kl}\psi_{-i\Lambda}^{(l)}); \\ \varphi \in D(\bar{H}_X), c_k \in \mathbf{C}\}, \\ H_{U,X} f = \bar{H}_X \varphi + i\Lambda \sum_{k=1}^{N} c_k(\psi_{i\Lambda}^{(k)} - \sum_{l=1}^{N} U_{kl}\psi_{-i\Lambda}^{(l)}), \end{aligned} \tag{26}$$

where U_{ij} denotes an arbitrary N-dimensional unitary matrix. Using Krein's formula, we can relate the Green's function of $H_{U,X}$ to $G^{(0)}$;

$$\begin{aligned} G_{U,X}(\vec{x}, \vec{y}; \omega) = G^{(0)}(\vec{x}, \vec{y}; \omega) \\ + \sum_{k,l=1}^{N} G^{(0)}(\vec{x}, \vec{x}_k; \omega) T(\omega)_{kl} G^{(0)}(\vec{x}_l, \vec{y}; \omega), \end{aligned} \tag{27}$$

where the transition matrix $T(\omega)$ should satisfy

$$\begin{aligned} [T(\omega)]_{kl}^{-1} - [T(\omega')]_{kl}^{-1} \\ = G^{(0)}(\vec{x}_k, \vec{x}_l; \omega') - G^{(0)}(\vec{x}_k, \vec{x}_l; \omega). \end{aligned} \tag{28}$$

Equation (28) indicates that it is sufficient to define the transition matrix for some fixed ω since then $T(\omega)$ for any ω follows from Eq.(28). Also note that Eq.(27) implies

$$T(\omega)^{\dagger} = T(\bar{\omega}). \tag{29}$$

The general form of $T(\omega)$ which satisfies Eqs.(28) and (29) is given by

$$T(\omega)^{-1} = A - G(\omega), \tag{30}$$

where

$$G(\omega)_{kl} = \begin{cases} \sum_{n=1}^{\infty} \varphi_n(\vec{x}_k)^2 (\frac{1}{\omega - E_n} + \frac{E_n}{E_n^2 + \Lambda^2}), \\ \qquad\qquad (k = l), \\ G^{(0)}(\vec{x}_k, \vec{x}_l, \omega), \quad (k \neq l), \end{cases} \tag{31}$$

and A is any N-dimensional Hermitian matrix. If A is not diagonal, different scatterers $\vec{x}_k$ are connected by the boundary conditions. On the other hand, if A is diagonal the point scatterers are independent, namely, one has separated boundary conditions at each $\vec{x}_k$. We here restrict ourselves to the latter which is important from a practical point of view. In this case, A can be parameterized as

$$A_{kl} = \delta_{kl} v_k^{-1}, \quad v_k \in \mathbf{R}. \tag{32}$$

One can regard v_k as the strength of the k-th scatterer. The eigenvalue of $H_{U,X}$ is determined by the poles of $T(\omega)$;

$$det(T(\omega)^{-1}) = 0, \tag{33}$$

which is reduced to Eq.(21) for $N = 1$.

A final remark is that one can show the relation

$$U = -{}^t[T(-i\Lambda)T(i\Lambda)^{-1}]. \tag{34}$$

Equation (34) indicates that the unitarity of U is equivalent to the fact that $T(i\Lambda)$ is a normal matrix.

IV. CONDITION FOR STRONG COUPLING

In this section, we discuss the condition for strong coupling under which point scatterers have a substantial effect on energy spectrum of the empty billiard. For this

purpose, we examine the energy-dependence of the inflection points of G in Eq.(20), based on a semi-quantitative argument suitable for examining the statistical properties of spectrum.

We first consider the case of a single scatterer. The first notice is that the average value of $\varphi_n(\vec{x}_1)^2$ among many n is independent of the energy;

$$\left\langle \varphi_n(\vec{x}_1)^2 \right\rangle_n \simeq 1/S. \tag{35}$$

We thus recognize from Eq.(22) that if $\omega_m \simeq E_m$ (resp. E_{m+1}) for some m, then $\psi_m \simeq \varphi_m$ (resp. $\psi_m \simeq \varphi_{m+1}$). This implies that a point scatterer distorts the wave function if the eigenvalue ω_m is located around the midpoint of the interval (E_m, E_{m+1}). For such ω_m, the value of G can be estimated by the principal integral as follows, since the contributions on the summation of G from the terms with $n \simeq m$ cancel each other;

$$G(\omega_m) \simeq g(\omega_m), \quad \omega_m \simeq \frac{E_m + E_{m+1}}{2}, \tag{36}$$

$$\begin{aligned} g(\omega) &= \left\langle \varphi_n(\vec{x}_1)^2 \right\rangle_n \rho_{av} P \int_0^\infty \left(\frac{1}{\omega - E} + \frac{E}{E^2 + \Lambda^2} \right) dE \\ &= \frac{M}{2\pi} \ln \frac{\omega}{\Lambda}. \end{aligned} \tag{37}$$

Here we have defined a continuous function $g(\omega)$ which behaves like an interpolation of the inflection points of G. Equation (36) indicates that the wave function mixing mainly occurs in the eigenstate with an eigenvalue such that

$$g(\omega_m) \simeq v_1^{-1}. \tag{38}$$

The "width" of the strong coupling region (allowable error of v_1^{-1} in Eq.(38)) is estimated by considering a linearized eigenvalue equation. Expanding G at $\omega_m \simeq (E_m + E_{m+1})/2$, we can rewrite the eigenvalue equation as

$$G'(\omega_m)(\omega - \omega_m) \simeq v^{-1} - G(\omega_m). \tag{39}$$

In order that Eq.(39) has a solution $\omega \simeq \omega_m$, the range of RHS has to be restricted to

$$\left| v^{-1} - G(\omega_m) \right| \lesssim \frac{\Delta}{2}, \tag{40}$$

$$\Delta \equiv |G'(\omega_m)|\, \rho_{av}^{-1}, \tag{41}$$

where we have defined the width Δ which is nothing but the variance of the linearized G on the interval (E_m, E_{m+1}). The magnitude of $|G'(\omega_m)|$ can be estimated as follows;

$$\begin{aligned} |G'(\omega_m)| &= \sum_{n=1}^{\infty} \left(\frac{\varphi_n(\vec{x}_1)}{\omega_m - E_n} \right)^2 \\ &\simeq \left\langle \varphi_n(\vec{x}_1)^2 \right\rangle_n \sum_{n=1}^{\infty} \frac{2}{\{(n - \frac{1}{2})\rho_{av}^{-1}\}^2} \\ &= 8 \left\langle \varphi_n(\vec{x}_1)^2 \right\rangle_n \rho_{av}^2 \sum_{n=1}^{\infty} \frac{1}{(2n-1)^2} \\ &= \pi^2 \left\langle \varphi_n(\vec{x}_1)^2 \right\rangle_n \rho_{av}^2. \end{aligned} \tag{42}$$

The second equality follows from the approximation that the unperturbed eigenvalues are distributed with a mean interval ρ_{av}^{-1} in the whole energy region. Noticing Eqs.(6) and (35), we obtain

$$\Delta \simeq \frac{\pi M}{2}, \tag{43}$$

which is independent of the energy ω. We can summarize the findings as follows; The effect of a point scatterer of coupling strength v_1 is substantial mainly in the eigenstates with eigenvalue ω such that

$$\left| v_1^{-1} - \frac{M}{2\pi} \ln \frac{\omega}{\Lambda} \right| \lesssim \frac{\Delta}{2} \simeq \frac{\pi M}{4}. \tag{44}$$

The condition (44) is generalized to the case of multiple scatterers. Equation (35), which is the main assumption in the above argument, is valid even for the perturbed eigenfunction (22). This allows us to repeat the above when the number of the point scatterers increases. We conclude that the k-th point scatterer with strength v_k affects the energy spectrum in the energy region such that

$$\left| v_k^{-1} - \frac{M}{2\pi} \ln \frac{\omega}{\Lambda} \right| \lesssim \frac{\pi M}{4}, \quad k = 1, \cdots, N. \tag{45}$$

It is worthy to emphasize that the strong coupling region shifts with a logarithmic dependence of energy. This indicates that the system recovers the integrability in the semiclassical (high-energy) limit for any strength v_k.

V. NUMERICAL EXAMPLE

TABLE I. Location of the point scatterers

k	x_k	y_k
1	0.6224826	0.2758356
2	0.8202505	0.4561782
3	0.1802603	0.6365209
4	0.3780281	0.8168635
5	0.5757960	0.2332624
6	0.7735638	0.4136051
7	0.1335736	0.5939477
8	0.3313415	0.7742904
9	0.5291093	0.1906893
10	0.7268772	0.3710320

In this section, we set the scale mass $\Lambda = 1$ without losing generality. This makes all physical quantities dimensionless. We consider a quantum particle with mass $M = 2\pi$ moving in a rectangular billiard with side-lengths $(l_x, l_y) = (\pi/3, 3/\pi)$, and hence $S = 1$. The average level density is $\rho_{av} = 1$, according to Eq.(6). The eigenvalue E_{n_x,n_y} and the corresponding eigenfunction φ_{n_x,n_y} are given by

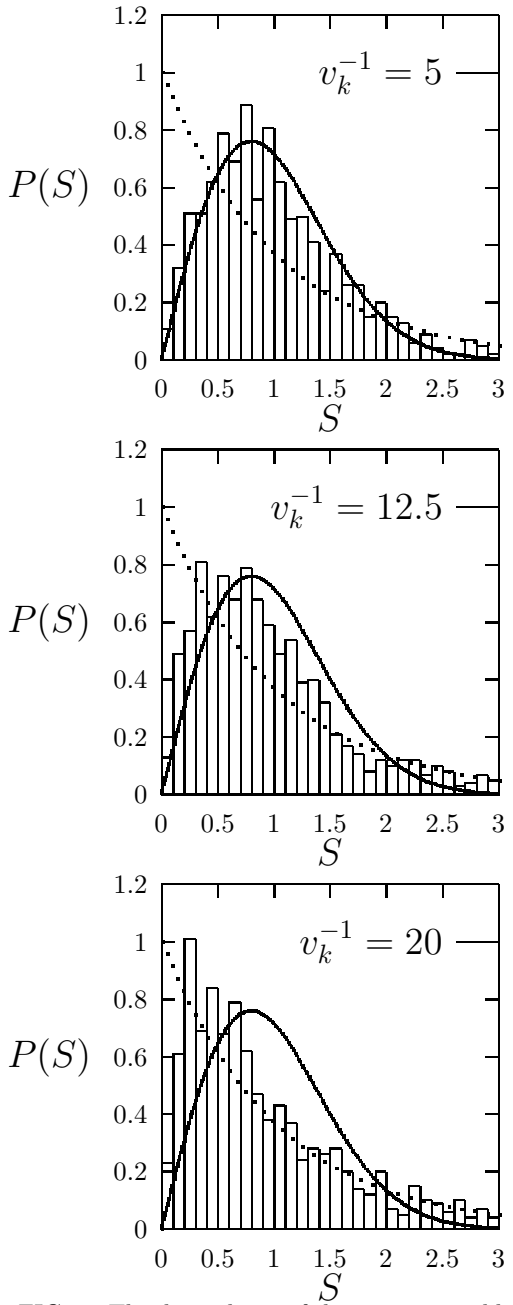

FIG. 1. The dependence of the nearest-neighbor level spacing distribution on the strength of the point scatterers. The number of the scatterers is $N = 5$ in all cases. The strength of all the scatterers is common. The statistics is taken among the eigenstates between ω_{100} and ω_{1100}. The solid (broken) line is the prediction of GOE (Poisson statistics).

$$E_{n_x,n_y} = \frac{1}{2M}\left\{\left(\frac{n_x\pi}{l_x}\right)^2 + \left(\frac{n_y\pi}{l_y}\right)^2\right\}, \tag{46}$$

$$\varphi_{n_x,n_y}(x,y) = \sqrt{\frac{4}{S}}\sin\frac{n_x\pi x}{l_x}\sin\frac{n_y\pi y}{l_y}, \tag{47}$$

respectively, $(n_x, n_y = 1, 2, \cdots)$. We obtain E_n and φ_n by arranging the double-indexed eigenvalues and eigenfunctions in ascending order of magnitude of E_{n_x,n_y}.

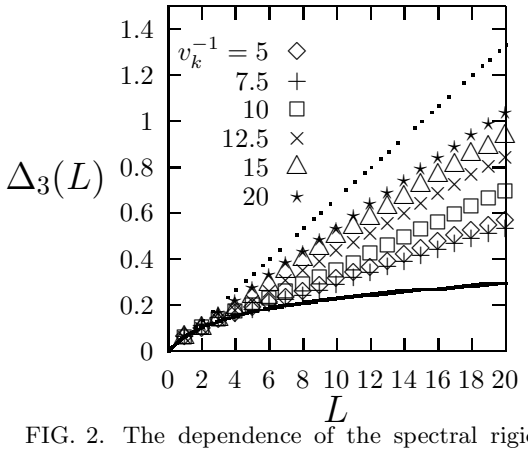

FIG. 2. The dependence of the spectral rigidity on the strength of the point scatterers. The other indications are the same as in Fig.1.

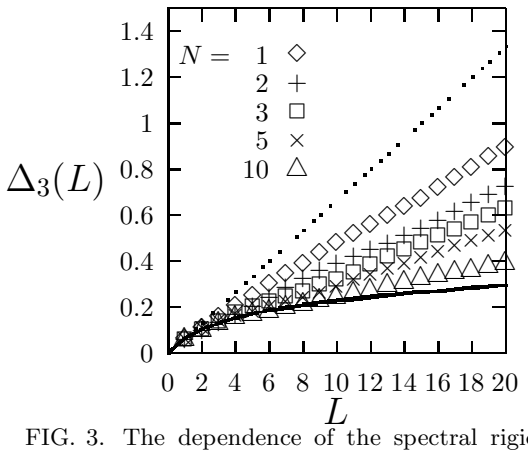

FIG. 3. The dependence of the spectral rigidity on the number of the point scatterers. The strength of all the scatterers is $v_k^{-1} = 7.5$.

We put several point scatterers inside the rectangle. The location of point scatterers, $\vec{x}_k = (x_k, y_k)$, is shown in Table I. The first N coordinates are used in case of the number of scatterers being N. It is expected from Eq.(45) that the k-th scatterer has a substantial effect on energy spectrum if its strength satisfies

$$\left|v_k^{-1} - \ln\omega\right| \lesssim \frac{\pi^2}{2} = 4.9348. \tag{48}$$

This is in fact the case, as seen from Fig.1 where the nearest-neighbor level spacing distribution $P(S)$ for three values of the strength of the scatterers is shown. The

number of point scatterers is $N = 5$ in all cases. The strength of all the scatterers is common. The statistics is taken within one thousand eigenvalues between $\omega_{100} = 110.3579$ and $\omega_{1100} = 1138.9682$. In this energy region, the chaotic spectrum is expected to appear for $v_k^{-1} \simeq 5 \sim 7$. The coincidence with the GOE prediction (solid line) is satisfactory for $v_k^{-1} = 5$. As v_k^{-1} increases, the level repulsion becomes weak and $P(S)$ shows intermediate between Poisson and GOE for $v_k^{-1} = 12.5$, as expected from Eq.(48). A further increase of v_k^{-1} makes the distribution approach the Poisson distribution (broken line), though there still remains the level repulsion even for $v_k^{-1} = 20$. A similar tendency can be observed in the spectral rigidity $\Delta_3(L)$, which Fig.2 shows for several values of v_k^{-1} under the same condition as in Fig.1. The $\Delta_3(L)$ statistics is close to the GOE prediction (solid line) in case of $v_k^{-1} = 5$ or 7.5. As v_k^{-1} increases, the gradual approach to the Poisson statistics (broken line) is observed. There still remains a considerable difference from the GOE prediction even in case of the maximal coupling. However, it tends to disappear as the number of scatterers increases. Figure 3 shows the dependence of the spectral rigidity on the number of the scatterers. The strength of all the scatterers is $v_k^{-1} = 7.5$, which is close to the maximal coupling strength. One can observe the gradual shift to the GOE prediction as the number of the scatterers increases.

VI. CONCLUSION

We have discussed the condition for the appearance of wave chaos in the two-dimensional quantum pseudointegrable billiards with multiple point scatterers inside. Chaotic spectrum appears if the condition of Eq.(45) is satisfied. It is described by a logarithmically energy-dependent strip with a constant width. The validity of our prediction is confirmed by numerical experiments with a rectangular billiard which contains multiple point obstacles inside. The degree of chaos depends on the number of the scatterers. We observe the GOE-like spectrum for $N = 10$ scatterers with the maximal coupling strength.

It should be stressed that, besides a fundamental aspect as a dynamical system, the quantum billiard with point interactions has a close relation to real systems. The quantum billiard is a natural starting point for examining the particle motion in microscopic bounded regions. The rapid progress in the microscopic or mesoscopic technology makes it possible to realize such settings. Real systems are, however, not free from small impurities which affect the particle motion inside. In the presence of a small amount of contamination, even a single-electron problem becomes unmanageable in an analytic manner. The modeling of the impurities with point interactions makes the problem easy to handle without changing essential dynamics. We hope that the current work serves as a guideline of the future research on the effect of impurities in mesoscopic devices.

[1] P.J. Richens and M.V. Berry, "Pseudointegrable systems in classical and quantum mechanics," Physica D, vol.2, pp.495–512, 1981.

[2] S. Albeverio and P. Šeba, "Wave chaos in quantum systems with point interaction," J. Stat. Phys., vol.64, nos.1/2, pp.369–383, 1991.

[3] T. Shigehara, "Conditions for the appearance of wave chaos in quantum singular systems with a pointlike scatterer," Phys. Rev. E, vol.50, no.6, pp.4357–4370, December, 1994.

[4] T. Shigehara and T. Cheon, "Spectral properties of three-dimensional quantum billiards with a pointlike scatterer," Phys. Rev. E, vol.55, no.6, pp.6832–6844, June, 1997.

[5] T. Shigehara, H. Mizoguchi, T. Mishima, and T. Cheon, "Wave chaos in quantum pseudointegrable billiards," Proc. International Symposium on Nonlinear Theory and its Applications, NOLTA'97, pp.441–444, Honolulu, Nov., 1997.

[6] O. Bohigas, "Random matrix theories and chaotic dynamics," in Les Houches Summer School Proceedings Session 52, ed. M.-J. Giannoni, A. Voros, and J. Zinn-Justin, pp.87–200, North-Holland, Amsterdam, 1989.

[7] M.L. Mehta, "Random matrices and the statistical theory of energy levels," Academic Press, New York, 1967, revised and enlarged edition, 1990.

[8] S. Albeverio, F. Gesztesy, R. Høegh-Krohn, and H. Holden, "Solvable models in quantum mechanics," Springer-Verlag, New York, 1988.

[9] J. Zorbas, "Perturbation of self-adjoint operators by Dirac distributions," J. Math. Phys., vol.21, no.4, pp.840–847, April, 1980.

Profile of the Authors

Takaomi Shigehara
email: sigehara@ics.saitama-u.ac.jp
http://www.me.ics.saitama-u.ac.jp/∼sigehara/
received the B.S, M.S and Ph.D. degrees in Physics from the University of Tokyo in 1983, 1985 and 1988, respectively. He is currently an Assistant Professor in the Department of Information and Computer Sciences at Saitama University. His research interests are quantum chaos, high-performance computing, and numerical analysis.

Hiroshi Mizoguchi
email: hm@ics.saitama-u.ac.jp
http://www.me.ics.saitama-u.ac.jp/∼hm/
received the B.E. degree in Mathematical Engineering in 1980, and the M.E. and Ph.D. degrees in Information Engineering in 1982 and 1985, respectively, from the University of Tokyo. He is currently an Associate Professor in the Department of Information and Computer Sciences at Saitama University. His research interests are vision processor system, robotics, and quantum chaos.

Taketoshi Mishima
email: misima@ics.saitama-u.ac.jp
http://www.me.ics.saitama-u.ac.jp/∼mishima/
received the B.E., M.E. and Ph.D. degrees in Electrical Engineering from Meiji University, Japan, in 1968, 1970 and 1973, respectively. He is currently a Professor in the Department of Information and Computer Sciences at Saitama University. His research interests are foundation of symbolic and algebraic computation, axiomatic logic system, mathematical pattern recognition, and quantum chaos.

Taksu Cheon
email: cheon@mech.kochi-tech.ac.jp
http://www.kochi-tech.ac.jp/∼cheon/
received the B.S., M.S. and Ph.D. degrees in Physics from the University of Tokyo in 1980, 1982 and 1985, respectively. He is currently an Associate Professor in the Laboratory of Physics at Kochi University of Technology. His research interests are quantum mechanics, chaos, and quantum chaos.